Indian Journal of Advances in Chemical Science

Article

Removal of Fluoride from Aqueous Solution by Adsorption on Perchloric Acid Cross-linked Calcium Alginate

Vijaya Yarramuthi*, Jaya Malathi Jagadeeson, Karuna Devi Rachapudi, Raja Kumar Challagundla

Department of Chemistry, Vikrama Simhapuri University, Nellore 524-003, Andhra Pradesh, India.

ABSTRACT

A novel biosorbent was developed by the crosslinking of an anionic biopolymer, calcium alginate (CA), with perchloric acid (PCA). The PCA cross-linked was characterized by Fourier-transform infrared, scanning electron microscopy (SEM), transmission electron microscopy, X-ray diffraction, and surface area analysis. Experimental parameters affecting the adsorption process such as pH, agitation time, concentration of adsorbate, and amount of adsorbent were studied. Langmuir and Freundlich isotherms were used to fit the experimental data. The best interpretation for the equilibrium data was given by the Langmuir isotherm. The maximum adsorption capacity for fluoride was 44 mg/g based on the Langmuir equation at a temperature of 28°C, a solution pH of 3.0, a adsorbent dosage of 0.7 g/100 mL, and a contact time of 120 min. The experimental data were analyzed using three sorption kinetic models, namely, pseudo-first-order, pseudo-second-order, and intraparticle diffusion model. Results show that the pseudo-second-order equation provides the best correlation for the adsorption process. The findings of the present study indicate that PCA can be successfully used for the removal of fluoride ions from aqueous solutions.

Key words: Perchloric acid, Defluoridation, Adsorption, Isotherms, Kinetics.

1. INTRODUCTION

Fluoride is widespread in the environment, water, air, vegetation, and the Earth's crust which can enter groundwater by natural process [1]. Fluoride in drinking water can be either beneficial or detrimental to health depending on its concentration. Fluoride in drinking water has a narrow beneficial concentration range in relation to human health. Small amounts in ingested water are usually considered to have a beneficial effect on the rate of occurrence of dental caries, particularly among children [2]. On the contrary, excess intake of fluoride leads to various diseases such as skeletal and teeth damage, paralysis of volition, osteoporosis, arthritis, brittle bones, cancer, infertility, brain damage, Alzheimer syndrome, and thyroid disorder [3,4]. The high concentration of fluoride can also interfere with carbohydrates, lipids, proteins, vitamins, and mineral metabolism [5]. Fluoride normally enters the environment and human body through water, food, drugs, cosmetics, etc. However, drinking water is the single major source of daily intake [6]. Due to the toxicity of fluoride and danger of overdosing, fluoridation of drinking water has been prohibited in many countries. Fluoride-containing wastewater is generated in various industries including glass and ceramic production, semiconductor manufacturing, pharmaceutical companies, electroplating, coal-fired power stations, beryllium extraction plants, brick and iron works, fertilizer manufacturing, and aluminum smelters [7]. According to the World Health Organization, the maximum allowable concentration of fluoride is 1.5 mg/L. For these reasons, the removal of the excess fluoride from waters and wastewater is important in terms of protection of public health and environment.

The most commonly adopted method in India, Nalgonda technique of community defluoridation, is based on precipitation process and is very efficient and cost effective. The process involves addition of aluminum sulfate with lime and sometimes bleaching powder, and lime is added 5% by weight [8]. The process is not very efficient. The major limitations of Nalgonda technique are daily addition of chemicals, large amount of sludge production, least effective with water having high total dissolved solid, and high hardness. A number of defluoridation techniques have been suggested for the removal of excess fluoride. For example, adsorption and biosorption [9-12], chemical precipitation including electrocoagulation/flotation process [13], membrane processes such as reverse osmosis, Nanofiltration, electrodialysis and Donnan dialysis [14-18], and other integrated process [19,20] were demonstrated effective method for removal fluoride. Each of technology has been found to be limited since the membrane processes often have high operational costs and the chemical precipitation may generate secondary wastes [13,15,16]. Among of these methods, adsorption technology as economical and efficient method and producing high-quality water has been widely studied. The major advantages of adsorption over other methods include low cost, high efficiency, minimization of the waste, and reuse of biosorbent. However, the efficiency of adsorption technique depends on the nature of adsorbents. Some of the adsorbents, namely, bleaching powder [21], quick lime [22], cashew nut shell [23], carboxylated cross-linked chitosan bead [24], modified cellulose [25], polymeric resins [26], activated carbon [27], metal loaded sorbents [28,29], Mg-Al-Zr triple-metal composite [30], porous MgO nanoplates [31],

*Corresponding Author:
E-mail: drvijayachem@gmail.com

ISSN NO: 2320-0898 (p); 2320-0928 (e)

DOI: 10.22607/IJACS.2018.602005

Received: 22nd February 2018;
Revised: 27th February 2018;
Accepted: 27rd February 2018

cerium immobilized cross-linked chitosan composite [32], zirconium-chitosan/graphene oxide membrane [33], and KOH-treated jamun (*Syzygium cumini*) seed [34] have been successfully employed for fluoride removal.

In recent years, research interest has been focused on increasing the sorption capacity of biomass through physical and chemical modification. All of these modifications were aimed to increase the density of the effective functional groups such as carboxylate, hydroxyl, sulfate, phosphate, amide, and amino groups on the biomass surface. In this study, perchloric acid (PCA) cross-linked calcium alginate (CA) was chosen as a biosorbent for the removal of fluoride ions from aqueous solutions. The primary objective of this research was to study the adsorption of fluoride from an aqueous solution by PCA cross-linked CA under kinetic and equilibrium studies. The secondary objective was to investigate the effect of pH, agitation time, concentration of adsorbate, and amount of adsorbent on the extent of adsorption. The tertiary objective included the fitting of the experimental data to the Langmuir and Freundlich adsorption isotherms and pseudo-first-order, pseudo-second-order, and intraparticle diffusion kinetic models. Further, the adsorbent was characterized by Fourier-transform infrared (FTIR), scanning electron microscopy (SEM), thermogravimetric analysis (TGA), X-ray diffraction (XRD), and surface area analysis.

2. MATERIALS AND METHODS

2.1. Chemicals

Sodium alginate was used to prepare the CA beads which were obtained from Loba Chemie (Mumbai, India). PCA, used for crosslinking of CA beads, was obtained from Ranbaxy Fine chemicals (New Delhi, India). Analytical reagent grade sodium fluoride, hydrochloric acid, and sodium hydroxide from S.D. Fine Chemicals (Mumbai, India) were used as a source of fluoride and for the pH adjustment. Total ionic strength adjustment buffer (TISAB) was used to eliminate the interference effect of complexing ions from fluoride solution which was obtained from Thermo Electron Corporation, Waltham, Massachusetts, USA.

2.2. Preparation of Fluoride Solution

The stock solution of 100 mg/L fluoride was prepared by dissolving 221 mg of anhydrous NaF in 1000 mL of double-distilled water, such that each mL of solution contains 1 mg of F^-. The exact concentration of fluoride ion solution is calculated on mass basis and expressed in terms of mg/L. The required lower concentrations 10, 15, and 20 mg/L are prepared by dilution of the stock solution. All precautions are taken to minimize the loss due to evaporation during the preparation of solutions and subsequent measurements. The stock solutions are prepared fresh for each experiment as the concentration of the stock solution may change on long standing.

2.3. Preparation of Biosorbent

Sodium alginate solution was prepared by dissolving and gently heating 40 g of alginate in 960 mL of water. The solution was then poured into 2% calcium chloride solution through the tip of the transfer pipette. The drops of sodium alginate solution gelled into 3.5 ± 0.1 mm diameter beads on contact with calcium chloride solution. The beads were kept in contact with calcium chloride solution for 4 h, which lead to the formation of insoluble and stable beads. Water-soluble sodium alginate was converted to water-insoluble CA beads using $CaCl_2$ solution. The beads were rinsed with double-distilled water and dried until the water was completely evaporated. It was observed that the size of the beads decreases on drying. Five different beads of the completely dried sample were taken randomly and the size of the each bead was measured using the micrometer screw gauge with an accuracy of ±0.01 mm. The average size of the bead was found to be 2.05 mm. 25 g of prepared CA beads were soaked in 500 mL of 0.05 M PCA for 4 h. PCA was cross-linked by CA beads due to chemical reaction. Then, the separated dried beads were used for the experiment.

2.4. Characterization of Adsorbent

FTIR Spectra (Nicolet-740, Perkin-Elmer-283B FTIR, USA) of PCA before and after adsorption of fluoride ions are recorded in the frequency range of 400–4000 cm^{-1}. The surface area of the PCA beads was measured by the single-point Brunauer–Emmett–Teller method with a thermal conductivity detector (Carlo Erba Soptomatic-1800, Milan, Italy) within the range 0.1–118.34 m^2/g with a sample size of 2.05 mm. The pycnomatic automatic temperature controller (ATC) was uniquely designed for the density measurement of solid and powder samples. Porosity is defined as the fraction of apparent volume of adsorbent that is attributed to the pores detected. The pore volume, density, and porosity of the adsorbent samples were measured with a pycnomatic ATC (Thermo Electron S.P.A., Milan, Italy). The surface morphology of the PCA before and after loaded with fluoride was visualized by SEM (JEOL JSM-5410, Japan). The PCA and fluoride-loaded PCA samples were also scanned using SEM, to examine the possible morphological changes in the surface. XRD analysis of before and after fluoride-loaded PCA samples was made using an X-ray powder diffractometer (Siemens D-5000, Germany) operating with the Cu Kα radiation (λ = 1.5406 Å). TG analysis of before and after fluoride-loaded PCA samples were recorded using Seiko TG/DTA analyzer in nitrogen atmosphere at a heating rate of 10°C/min over a temperature range of 25–700°C.

2.5. Batch Adsorption Studies

Biosorption adsorption experiments were carried out to examine the effects of contact time, adsorbent dose, initial fluoride concentration, and solution of pH on the adsorption performance of PCA and to obtain equilibrium and kinetic data. The stock solutions were diluted to required concentrations (10, 15, and 20 mg/L). Batch adsorption experiments were performed by agitating specified amount of adsorbent in 100 mL of fluoride solution of desired concentrations at varying pH in 125 mL stopper bottles. The reaction mixture was agitated at 200 rpm for a known period of time at room temperature in a mechanical shaker. After selected time intervals, the solutions were filtered and the liquid samples collected and analyzed for residual fluoride concentration using an ion selective electrode. TISAB was used as a TISAB during analysis. The percentage adsorption (%) and amount of adsorption (q_e) were calculated according to the following equations:

$$\% \text{ Removal} = \left(\frac{C_i - C_e}{C_i} \right) 100 \quad (1)$$

$$q_e = \left(\frac{C_i - C_e}{M} \right) V \quad (2)$$

Where C_i and C_e are the liquid phase concentration of ions initially and at equilibrium (mg/L), respectively. V is the volume of the fluoride solution (L), and M is the mass of the dry adsorbent used (g).

3. RESULTS AND DISCUSSION

3.1. Characterization of Adsorbent

3.1.1. FTIR analysis

FTIR spectra obtained for PCA and PCA loaded with fluoride demonstrate the sorption of fluoride on PCA surface. Table 1 represents FTIR spectra peaks for different functional groups present on PCA before and after

Table 1: Function groups observed on PCA biosorbent before and after fluoride sorption by FTIR spectroscopy.

PCA (cm^{-1})	PCA loaded with fluoride (cm–1)	Bonds indicative of
3430	3431	OH (hydroxyl and carbonyl groups) and N-H stretching
2936	2935	Asymmetric vibrations of CH
-	2871	C-H stretches (aldehyde)
1650	1643	C=O stretching
1463	1468	OH bonds
-	1077	-C-F stretch
873	873	Plane deformation
619	619	
-	747	O-H-F stretching

PCA: Perchloric acid, FTIR: Fourier-transform infrared

fluoride adsorption. In the present study, FTIR spectra mainly stress on the mechanism of fluoride sorption on PCA surface. When CA treated with PCA, the hydroxyl functional groups present on the alginate surface particularly oxidize to yield aldehyde functional groups. The stretching frequencies at 1643 cm^{-1} along with 2871 cm^{-1} clearly indicate the presence of aldehyde functional groups (1643 cm^{-1} –C=O; 2871 cm^{-1} sp^2 hybridized C-H). The remaining adsorption peaks were usually denoted the alginate functional groups such as -CH2, -COO, OH, and NH. 3430 and 3431 cm^{-1} broad bands in PCA before and after loaded fluoride, respectively, denote the OH stretching mode. Aliphatic -CH2, CH, and >CH2 were showed their corresponding peaks at 2936 and 2935 cm^{-1} in PCA before and after loaded fluoride, respectively. The fluoride adsorption on PCA also can be interpreted by the peak observed at 1077 cm^{-1} which is a stretching frequency of C-F. The new band appeared at 747 cm^{-1} in fluoride loaded with PCA corresponds to O-H-F hydrogen bonding confirmed the adsorption of fluoride on PCA. Therefore, PCA oxidizes CA to give aldehyde functional groups which can bond with fluoride ions to adsorb fluoride on PCA.

3.1.2. Surface area analysis

It is understood from the data in Table 2 that the internal pores of PCA beads are having small volume, which may be surrounded by void particles, nevertheless, they contribute to the much of the adsorption of the fluoride ions. It is well-known fact that the pore structure of plant and animal tissues which are of vital importance are formed fulfilling stringent conditions determined by natural processes of cell division, self-organization, etc., whose processes are yet to be understood clearly. The PCA showed higher percentage of porosity, which means that higher pore volume as well as more number of pores are available for adsorption of fluoride ions. Thus, the porosity is one of the characteristics that decide the strength of the adsorbent to adsorb the fluoride ions from the liquids.

3.1.3. SEM Studies

Typical surface morphologies of PCA beads before and after fluoride sorption are shown in Figure 1. It is evident from the surface, SEM micrographs that PCA beads before fluoride adsorption show some cracks on the outer surface (Figure 1a), but on fluoride loading, the biosorbent surface is somewhat non-uniform and the biosorbent became more brittle as shown in Figure 1b. The surface morphology and texture of fluoride-loaded sorbent were completely different from fluoride-unloaded sorbent. Figure 1b describes the surface characteristics and morphology of the adsorbent after their exposure to fluoride solution. It can be observed that there is a change in the morphology of the adsorbents after fluoride sorption. Surface morphological studies revealed that the process of fluoride sorption on PCA beads was predominantly surface phenomenon.

3.1.4. XRD studies

XRD studies provide information on the nature of the compound as well as on the spacing between the polymer beads. XRD pattern of PCA is shown before and after adsorption in Figure 2. From Figure 2a, it was observed that the PCA beads before adsorption are in close compaction with one another and thus a reduction in the cluster space may be encountered. The effective d-spacing (d) gives an indication of cluster space existing in the polymer before and after adsorption. The XRD of PCA before adsorption as shown in Figure 2a have no sharp peaks indicating the amorphous nature of the sorbent. The XRD spectra of PCA beads after adsorption (Figure 2b) exhibit a broad peak at $2\theta = 10^{o}$, which may be due to the intermolecular interaction such as the formation of weak hydrogen bonding between alginates and fluoride.

3.1.5. TGA studies

The TGA curves of the PCA and fluoride-loaded PCA beads are shown in Figure 3. The TGA curve of PCA (Figure 3a) shows the beginning of weight loss at 230°C followed by a final decomposition at 310°C. Figure 3b shows that fluoride-loaded PCA begins to undergo a weight loss starting at 210°C followed by the final decomposition at 300°C. This observation indicates that there is no considerable difference in thermal stability of PCA before and after fluoride treatment. From the TGA analysis of the biosorbent, it may be concluded that the fluoride-loaded PCA could be used even at higher temperatures in water treatment.

3.2. Effect of Initial pH

The role of pH is a major factor controlling adsorption at the water-adsorbent interface [12]. The effect of pH on removal of fluoride was studied over the pH range of 1–10 with 10 mg/L as the initial fluoride concentration at room temperature and results are shown in Figure 4. It can be seen from the Figure 4 that the adsorption capacity of fluoride was changed; it first increased to 1.44 mg/g (72%) at pH 3.0 and then slightly decreased to 1.24 mg/g (62%) at pH 4.0. After that, the adsorption capacity dramatically decreased, and the adsorbent exhibited negligible adsorption (0.50 mg/g [20%]) at pH 10.0. The maximum adsorption (72%) was obtained at pH value of 3.0. The lower defluoridation efficiency at pH below 3.0 is possible due to protonation of fluoride. This result could be attributed to the formation of weakly ionized hydrofluoric acid [35]. The decrease of defluoridation can be explained by the change in surface charge of the adsorbent. In acidic medium, the surface is highly protonated, and therefore, the observed maximum fluoride removal is attributed to the gradual increase in attractive forces between the positively charged surface and negatively charged fluoride ions. The lower defluoridation capacity in alkaline medium can be explained by the fact that in alkali the surface acquires

Table 2: Surface properties of PCA beads

Property	PCA cross-linked CA
Surface area (m^2/g)	101.25
Porosity (%)	33.40
Pore volume (cm^3/g)	0.37
Pore diameter (cm/g)	0.71
Density (g/cm^3)	2.01

PCA: Perchloric acid, CA: Calcium alginate

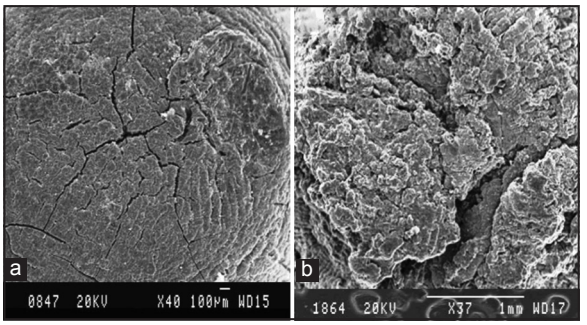

Figure 1: Scanning electron microscopy images of (a) perchloric acid (PCA) and (b) PCA loaded with fluoride.

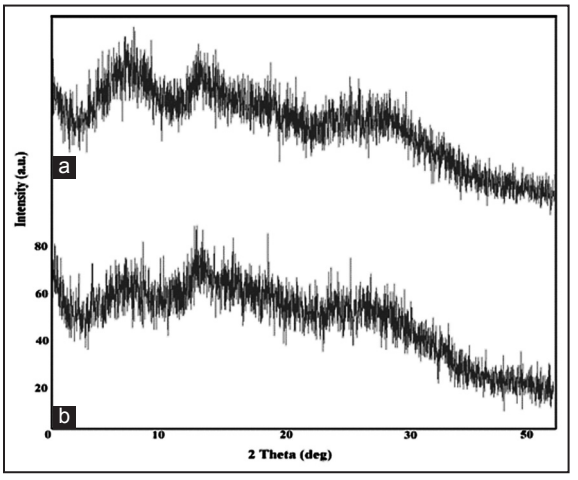

Figure 2: Power X-ray diffraction spectra of (a) perchloric acid (PCA) and (b) PCA-loaded with fluoride.

a negative charge and hence there is repulsion between the negatively charged surface and fluoride [36]. Therefore, all the adsorption experiments were carried out at this pH value.

3.3. Effect of Contact Time

The effect of contact time on the extent of adsorption of fluoride at different concentrations is shown in Figure 5. The extent of adsorption increases with time and attained equilibrium for all the concentrations of fluoride studied (10, 15, and 20 mg/L) at 120 min. After the equilibrium period, the amount of fluoride adsorbed did not change significantly with time. The amount of fluoride adsorbed versus time curves is smooth and continuous. The changes in the rate of removal might be due to the fact that initially all adsorbent sites are vacant and the solute concentration gradient is high. Later, the fluoride uptake rate by adsorbent has decreased significantly, due to the decrease in a number of adsorption sites. Decreased removal rate, particularly, toward the end of experiment, indicates the possible monolayer of

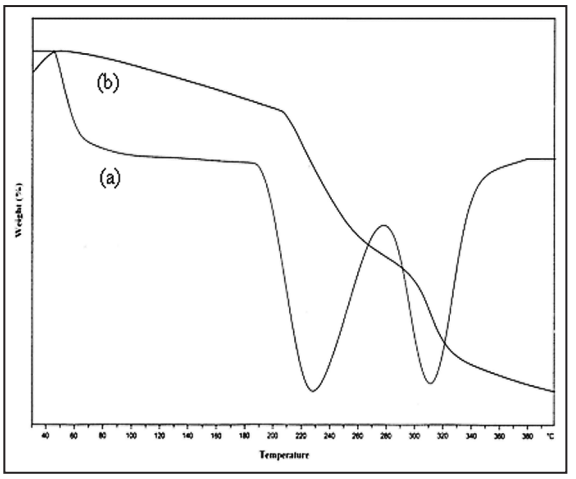

Figure 3: Thermogravimetric analysis curves of (a) perchloric acid (PCA) and (b) PCA loaded with fluoride.

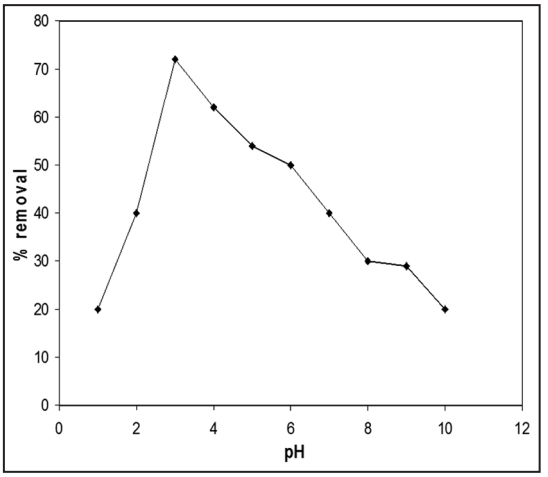

Figure 4: Effect of pH on adsorption of fluoride on perchloric acid (initial fluoride concentration: 10 mg/L; pH 1–10; adsorbent dose: 0.7 g/100 mL; temperature: 28°C; contact time: 120 min).

fluoride ions on the outer surface, pores of both the adsorbents, and pore diffusion onto inner surface of adsorbent particles through the film due to continuous shaking maintained during the experiment.

3.4. Adsorption Kinetics

To examine the controlling mechanism of adsorption process such as mass transfer and chemical reaction, pseudo-first-order, pseudo-second-order, and intraparticle diffusion kinetic equations were used to test the experimental data. The pseudo-first-order kinetic model was suggested by Lagergren [37] for the adsorption of solid/liquid systems and its formula is given as follows:

$$\log(q_e - q_t) = \log q_e - \frac{K_1}{2.303} t \quad (3)$$

Where q_e and q_t are the amounts of adsorbate adsorbed (mg/g) at equilibrium and at any time, t (min), respectively, and K_1 is the rate constant of pseudo-first-order adsorption (min^{-1}).

The plot of log (q_e-q_t) versus t (figure not shown) gave a straight line for pseudo-first-order adsorption kinetics to obtain the rate parameters. The values of K_1, the calculated adsorption capacity, $q_{e,cal}$, and correlation coefficients, R^2, obtained from the plots for adsorption of fluoride on PCA were presented in Table 3. The values of R^2 were

relatively small. It was also observed that the $q_{e,cal}$ values calculated from the Lagergren plots did not agree with the experimental q_e values, $q_{e,exp}$ (Table 3). This indicated that the adsorption of fluoride on PCA did not follow the pseudo-first-order kinetics.

The kinetic data were further analyzed using Ho's pseudo-second-order kinetics model [38]. This model is based on the assumption that the sorption follows second-order chemisorption. It can be expressed as:

$$\frac{t}{q_t}=\frac{1}{K_2 q_e^2}+\frac{1}{q_e}t \quad (4)$$

Where K_2 (g/mg min) is the rate constant of pseudo-second-order equation, q_t (mg/g) is the amount of adsorption time t (min), and q_e is the amount of adsorption equilibrium (mg/g). The value of q_e (1/slope) and K_2 (slope^2/intercept) of the pseudo-second-order equation can be found out experimentally by plotting t/q_t versus t (Figure 6). The fitness of the data and the values of q_e and K_2 were obtained from the plots of t/q_t versus t for fluoride sorption, and various initial fluoride concentrations, namely, 10, 15, and 20 mg/L of PCA are presented in Table 3. It is clear from these results that the R^2 values are very high (in the range of 0.995–0.999) for fluoride adsorption. In addition, the theoretical $q_{e,cal}$ values were closer to the experimental $q_{e,exp}$ values (Table 3). In the view of these results, it can be said that the pseudo-second-order kinetic model provided a good correlation for the adsorption of fluoride on PCA in contrast to the pseudo-first-order.

The results were also analyzed in terms of intraparticle diffusion model to investigate whether the intraparticle diffusion was the rate controlling step in adsorption of fluoride on PCA. The mathematical expression for the intraparticle diffusion model [39] might be represented as,

$$q_t = K_{id}t^{1/2}+C \quad (5)$$

Where q_e (mg/g) is the amount adsorbed at time t, C (mg/g) is the intercept, and K_{id} (mg/g min$^{-1/2}$) is the intraparticle diffusion rate constant. Figure 7 shows the amount of fluoride sorbed versus $t^{1/2}$ at three different concentrations with a fixed adsorbent dose. The plots in the figure are multilinear with three distinct regions indicating three different kinetic mechanisms. The initial curved region corresponds to the external surface uptake, the second stage relates the gradual uptake reflecting intraparticle diffusion as the rate-limiting step, and final plateau region indicates equilibrium uptake. Based on the results, it may be concluded that the intraparticle diffusion is not the only rate-determining step [40]. The K_{id} values were obtained from the slope of the linear portions of the curve at different initial fluoride concentrations and have been indicated in Table 3.

3.5. Equilibrium Modeling

The analysis of adsorption data is important to develop an equation which accurately represents the results and which could be used for design purpose. The most commonly applied isotherms, in solid/liquid system, are Langmuir and Freundlich isotherms. The Langmuir equation is chosen for the estimation of maximum adsorption capacity corresponding to complete monolayer coverage on the biosorbent surface. The Freundlich model is chosen to estimate the adsorption intensity of the sorbent toward the biomass. In this work, attempts have been made to analyze adsorption by these two models. The linear regression was used to determine the most fitted model among the two adsorption isotherms.

3.5.1. Langmuir isotherm

Langmuir [41] isotherm model can be represented in the form of equation:

$$\frac{1}{q_e}=\frac{1}{q_m b C_e}+\frac{1}{q_m} \quad (6)$$

Where q_m is the amount of adsorbate at complete monolayer coverage (mg/g), which gives the maximum sorption capacity of sorbent, and b (L/mg) is the Langmuir isotherm constant that rates to the energy of adsorption. The results show that experimental data are in good agreement with the Langmuir isotherm with high correlation as shown in Table 4. In this table, the values of q_m and b were evaluated from slope and intercept of the straight line for the $1/C_e$ versus $1/q_e$ plot, respectively.

The type of the Langmuir could be predicted based on whether the adsorption was favorable or unfavorable in terms of equilibrium parameter or dimensionless constant separation factor R_L, which has been defined and disclosed by the following equation.

$$R_L=\frac{1}{1+bC_o} \quad (7)$$

Where b is the Langmuir isotherm constant and C_o is the initial concentration of fluoride (mg/L).

The parameter R_L indicates the shape of the isotherm and nature of the adsorption process (R_L>1: Unfavorable; R_L=1: Linear; 0<R_L<1: Favorable; and R_L=0: Irreversible) [42]. The R_L values between 0 and 1 indicate favorable adsorption for all the initial concentrations.

On the other hand, Table 5 presents the comparison of adsorption capacity and other parameters of PCA for the removal of fluoride with

Table 3: Kinetic models for adsorption of fluoride on PCA associated with correlation coefficient.

C_o	$q_{e.exp}$ (mg/g)	Pseudo-first-order			Pseudo-second-order			Intraparticle diffusion		
		K_1 (1/min)	R^2	$q_{e.cal}$ (mg/g)	K^2 (g/mg min)	R^2	$q_{e.cal}$ (mg/g)	K_{id} (mg/(g min$^{-0.5}$))	C	R^2
10	1.648	0.0022	0.964	0.785	0.026	0.995	1.739	0.130	0.232	0.922
15	2.732	0.0014	0.988	0.952	0.025	0.998	2.847	0.202	0.537	0.860
20	3.694	0.0034	0.926	0.864	0.027	0.999	3.828	0.266	0.935	0.792

PCA: Perchloric acid

Table 4: Isotherms for adsorption of fluoride on PCA associated with correlation coefficient and Chi-square analysis.

Adsorbent	Langmuir				Freundlich				
	q_m (mg/g)	b (L/mg)	R^2	χ^2	K_f (mg/g)	1/n (L/mg)	n	R^2	χ^2
PCA	44	0.010	0.998	31	0.493	0.900	1.111	0.973	106

PCA: Perchloric acid

those of different adsorbents reported in literature [43-52]. Based on this table, it can be concluded that the PCA has an important potential for the removal of fluoride ions from aqueous solution.

3.5.2. Freundlich isotherm

The linear form of Freundlich [53] isotherm is represented by the equation,

$$\log q_e = \log K_f + \frac{1}{n}\log C_e \quad (8)$$

Where q_e is the amount of fluoride adsorbed per unit weight of the sorbent (mg/g), C_e is the equilibrium concentration of fluoride in solution (mg/L), K_f is a measure of adsorption capacity, and 1/n is the adsorption intensity. The values of 1/n and K_f of the sorbent were calculated from the slope and the intercept of the linear plot of log C_e versus log q_e and are listed in Table 4. The magnitude of the exponent 1/n lying between 0 to 1 and the value of n > 1 indicate favorable conditions for adsorption.

3.6. Chi-square Analysis

To identify a suitable isotherm model for the sorption of fluoride on PCA, this analysis has been carried out. The Chi-square test statistic is basically the sum of the squares of the differences between the experimental data and data obtained by calculating from models, with each squared difference divided by the corresponding data obtained by calculating from the models. The mathematical statement of Chi-square can be given as:

$$\chi^2 = \sum\left(\frac{(q_e - q_{e,m})^2}{q_{e,m}}\right) \quad (9)$$

Where $q_{e,m}$ is equilibrium capacity calculated from the model (mg/g) and q_e is the experimental data of the equilibrium capacity (mg/g). If data from the model are similar to the experimental data, χ^2 will be a small number, while if they differ, χ^2 will be a larger number. Therefore, it is necessary to analyze the data set using the non-linear Chi-square test to confirm the best-fit isotherm for the sorption system [26]. The χ^2 values of both the isotherms are comparable, and hence, the adsorption of fluoride on PCA follows both Freundlich and Langmuir isotherms and better fits to Langmuir as its χ^2 value is less than that of Freundlich model as presented in Table 4.

3.7. Effect of Adsorbent Dose

To examine the effect of the dosage on the percentage fluoride removal, studies were conducted with a fixed time, 10 mg/L as initial fluoride concentration at pH 3.0 and room temperature. The effect of percentage fluoride removal on sorbent dosage as shown in Figure 8 demonstrates that there is an increase in percentage fluoride removal with the increase of dosage of beads as expected. The extent of fluoride removal by PCA is 30% (3.00 mg/g) with 0.10 g/100 mL of adsorbent dose, while it was greatly increased to 72% (1.20 mg/g) with 0.6 g/100 mL of adsorbent. However, when the adsorbent was about 0.70 g/100 mL, the percent removal increased to 82% (1.17 mg/g) only. The removal efficiency increases up to an optimum dose of 0.10–0.70 g of sorbent. This is expected due to the fact that the higher dose of adsorbent in the solution results in greater availability of adsorption sites for the ions.

4. CONCLUSION

In this study, PCA beads were successfully used as a biosorbing agent for the removal of fluoride ions from aqueous solution. The batch study parameters, pH of solution, agitation time, concentration of adsorbate, and amount of adsorbent were found to be effective on the adsorption efficiency of fluoride. The maximum adsorption capacity of PCA beads were determined as 44 mg/g for fluoride, at optimum conditions of pH 3.0, adsorbent dosage of 0.7 g/100 mL, contact time of 120 min, and solution temperature of 28°C. Further, the biosorbent

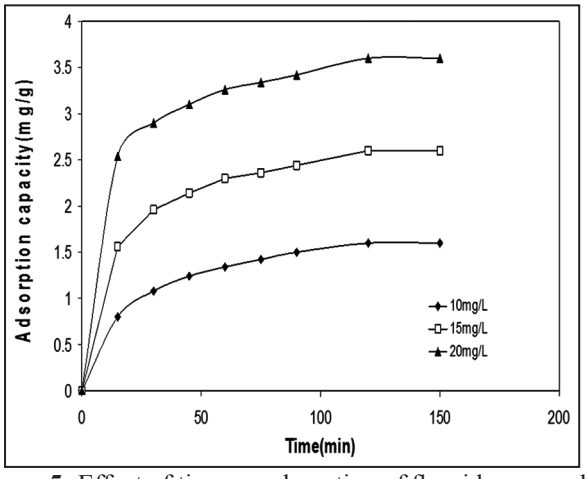

Figure 5: Effect of time on adsorption of fluoride on perchloric acid (initial fluoride concentrations: 10, 15, and 20 mg/L; adsorbent dose: 0.7 g/100 mL; pH: 3; temperature: 28°C; contact time: 15–150 min).

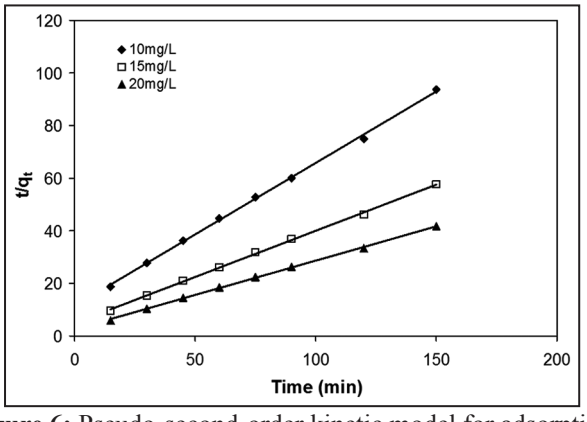

Figure 6: Pseudo-second-order kinetic model for adsorption of fluoride on perchloric acid (initial fluoride concentrations: 10, 15, and 20 mg/L; adsorbent dose: 0.7g/100 mL; temperature: 28°C; contact time: 15–150 min).

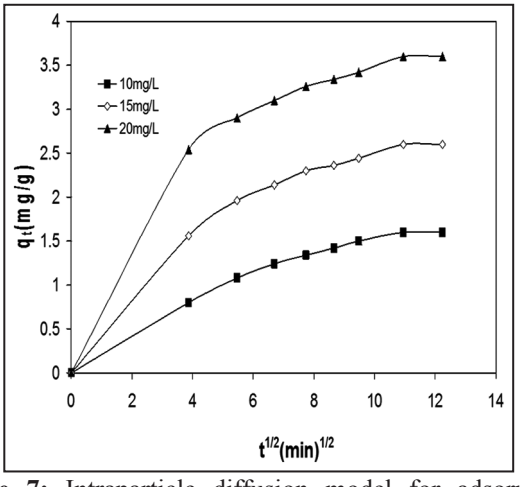

Figure 7: Intraparticle diffusion model for adsorption of fluoride on perchloric acid (initial fluoride concentrations: 10, 15, and 20 mg/L; adsorbent dose: 0.7 g/100 mL; temperature: 28°C; contact time: 15–150 min).

Table 5: Comparison of the adsorption capacity and other parameters of PCA with different adsorbents.

Adsorbent	Adsorption capacity (mg/g)	Concentration range (mg/L)	Contact time (h)	pH	References
Calcium chloride modified natural zeolite	1.766	25-100	6	6.0	[43]
Manganese oxide-coated alumina	2.851	2.5-30	3	7.0	[44]
Lanthanum incorporated chitosan beads	4.7	5.34	24	5.0	[45]
COCA	7.770	10	24	-	[46]
Chitosan-based mesoporous	8.264	5.0	24	-	[47]
$KMnO_4$-modified carbon	15.9	20	3	2.0	[48]
Glass-derived hydroxyapatite (G-HAP)	17.34	100	12	6.72	[49]
Neodymium-modified chitosan	22.380	10-100	24	7.0	[50]
Zirconium ion impregnated coconut fiber	40.016	-	6	4.0	[51]
Modified attapulgite	41.5	20-200	48	7.0	[52]
PCA cross-linked CA	44	10-20	2	3.0	Present study

COCA: Copper oxide coated alumina, PCA: Perchloric acid, CA: Calcium alginate

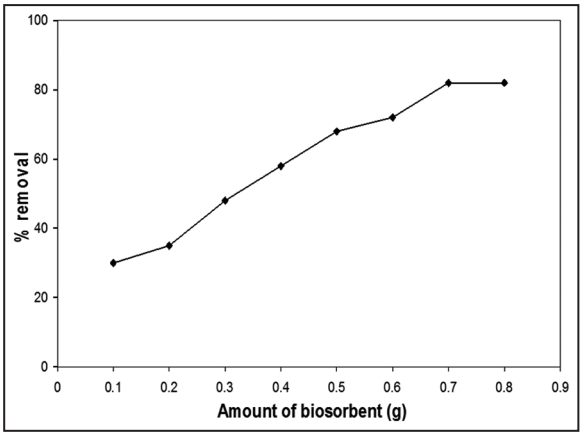

Figure 8: Effect of adsorbent dose on adsorption of fluoride on perchloric acid (initial fluoride concentration: 10 mg/L; adsorbent dose: 0.1–0.8 g/100 mL; pH: 3; temperature: 28°C; contact time: 120 min).

was characterized by FTIR, SEM, transmission electron microscopy, XRD, and surface area analysis. The adsorption equilibrium was better described by the Langmuir isotherm than the Freundlich equation. The kinetic studies revealed that the adsorption process followed well the pseudo-second-order kinetic model. All these results suggest that PCA beads can be used effectively for the removal of fluoride from aqueous solution.

5. REFERENCES

1. H. Paudyal, B. Pangeni, K. Inoue, H. Kawakita, K. Ohto, H. Harada, S. Alam, (2011) Adsorptive removal of fluoride from aqueous solution using orange waste loaded with multi-valent metal ion, ***Journal of Hazardous Materials,*** **192:** 676-682.
2. M. Mahramanlioglu, I. Kizilcikli, I. O. Bicer, (2002) Adsorption of fluoride from aqueous solution by acid treated spent bleaching earth, ***Journal of Fluorine Chemistry***, **115:** 41-47.
3. N. J. Chinoy, (1991) Effects of fluoride on physiology of animals and human beings, ***Indian Journal of Environment and Toxicology***, **1:** 17-32.
4. P. T. C. Harrison, (2005) Fluoride in water: A UK perspective, ***Journal of Fluorine Chemistry***, **126:** 1448-1456.
5. B. Kemer, D. Ozdes, A. Gundogdu, V. N. Bulut, C. Duran, M. Soylak, (2009) Removal of fluoride ions from aqueous solution by waste mud, ***Journal of Hazardous Materials***, **168:** 888-894.
6. N. Viswanathan, C. S. Sundaram, S. Meenakshi, (2009) Development of multifunctional chitosan beads for fluoride removal, ***Journal of Hazardous Materials***, **167:** 325-331.
7. F. Shen, X. Chen, P. Gao, G. Chen. (2003) Electrochemical removal of fluoride ions from industrial wastewater, ***Chemical Engineering Science***, **58:** 987-993.
8. B. V. Apparao, S. Meenakshi, G. Karthikayan, (1990) Nalgonda technique of defluoridation of water, ***Indian Journal of Environmental Protection***, **10(4):** 292-298.
9. X. Fan, D. J. Parker, M. D. Smith, (2003) Adsorption kinetics of fluoride on low cost materials, ***Water Research***, **37:** 4929-4937.
10. M. S. Onyango, Y. Kojima, O. Aoyi, E. C. Bernardo, H. Matsuda, (2004) Adsorption equilibrium modeling and solution chemistry dependence of fluoride removal from water by trivalent-cation-exchanged zeolite F-9, ***Journal of Colloid and Interface Science***, **279:** 341-350.
11. Y. H. Li, S. Wang, X. Zhang, J. Wei, C. Zu, Z. Luan, D. Wu. (2003) Adsorption of fluoride from water by aligned carbon nanotubes, ***Materials Research Bulletin***, **38:** 469-476.
12. A. K. Yadav, C. P. Kaushik, A. K. Haritash, A. Kansal, N. Rani, (2006) Defluoridation of groundwater using brick powder as an adsorbent, ***Journal of Hazardous Materials***, **128:** 289-293.
13. M. M. Emamjomeh, M. Sivakumar, (2006) An empirical model for defluoridation by batch monopolar electrocoagulation/flotation (ECF) process, ***Journal of Hazardous Materials***, **131:** 118-125.
14. C. David, M. C. Herbert, (1998) 65,000 GPD fluoride removal membrane systems in Lakeland, California, USA, ***Desalination***, **117:** 19-35.
15. K. Hu, M. D. James, (2006) Nanofiltration membrane performance on fluoride removal from water, ***Journal of Membrane Science***, **279:** 529-538.
16. P. I. Ndiaye, P. Moulin, L. Domingwez, J. C. Millet, F. Charbit, (2005) Removal of fluoride from electronic industrial effluent by RO membrane separation, ***Desalination***, **173:** 25-32.
17. T. Ruiz, F. Persin, M. Hichour, J. Sandeaue, (2003) Modelisation of fluoride removal in Donnan dialysis, ***Journal of Membrane Science***, **212:** 113-121.
18. M. Hichour, F. Persin, J. Sandeaux, C. Gavach, (2000) Fluoride

removal from waters by Donnan dialysis, ***Separation and Purification Technology***, **18:** 1-11.
19. N. Parthasarathy, J. Buffle, W. Haerdi, (1986) Combined use of calcium salts and polymeric aluminum hydroxide for defluoridation of wastewaters, ***Water Research***, **20:** 443-448.
20. M. Hichour, F. Persin, J. Sandeaux, C. Gavach, (1999) Fluoride removal from by diluted solution by donnan dialysis with anion-exchange membrane, ***Desalination***, **122:** 53-62.
21. S. Kagne, S. Jagtap, D. Thakare, S. Devotta, S. S. Rayalu, (2009) Bleaching powder: A versatile adsorbent for the removal of fluoride from aqueous solution, ***Desalination***, **243:** 22-31.
22. M. Islam, R. K. Patel, (2007) Evaluation of removal of fluoride from aqueous solution using quick lime, ***Journal of Hazardous Materials***, **143:** 303-310.
23. G. Alagumuthu, M. Rajan. (2010) Equilibrium kinetics of adsorption of fluoride on to zirconium-impregnated cashew nut shell carbon, ***Chemical Engineering Journal***, **158:** 451-457.
24. N. Viswanathan, C. S. Sundaram, S. Meenakshi, (2009) Sorption behavior of fluoride on carboxylated cross-linked chitosan beads, ***Colloids and Surfaces B: Biointerfaces***, **68:** 48-54.
25. Y. Zhao, X. Li, L. Liu, F. Chen. (2008) Fluoride removal by Fe(III)-loaded ligand exchange cotton cellulose adsorbent from drinking water, ***Carbohydrate Polymers***, **72:** 144-150.
26. S. Meenakshi, N. Viswanathan, (2007) Identification of selective ion exchange resin for fluoride sorption, ***Journal of Colloid and Interface Science***, **308:** 438-450.
27. D. Mohan, K. P. Singh, V. K. Singh, (2008) Wastewater treatment using low cost activated carbons derived from agricultural byproducts-a case study, ***Journal of Hazardous Materials***, **152:** 1045-1053.
28. N. Viswanathan, S. Meenakshi, (2009) Role of metal ion incorporation in ion exchange resin on the selectivity of fluoride, ***Journal of Hazardous Materials*****, 162:** 920-930.
29. N. Viswanathan, S. Meenakshi, (2008) Effect of metal ion loaded in a resin towards fluoride retention, ***Journal of Fluorine Chemistry***, **129:** 645-653.
30. M. Wang, X. Yu, C. Yang, X. Yang, M. Lin, L. Guan, M. Ge, (2017) Removal of fluoride from aqueous solution by Mg-Al-Zr triple-metal composite, ***Chemical Engineering Journal***, **322:** 246-253.
31. Z. Jin, Y. Jia, K. S. Zhang, L. T. Kong, B. Sun, W. Shen, F. L. Meng, J. H. Liu, (2016) Effective removal of fluoride by porous MgO nanoplates and its adsorption mechanism, ***Journal of Alloys and Compounds***, **675:** 292-300.
32. T. Zhu, T. Zhu, J. Gao, L. Zhang, W. Zhang, (2017) Enhanced adsorption of fluoride by cerium immobilized cross-linked chitosan composite, ***Journal of Fluorine Chemistry***, **194:** 80-88.
33. J. Zhang, N. Chen, P. Su, M. Li, C. Feng, (2017) Fluoride removal from aqueous solution by zirconium-chitosan/graphene oxide membrane, ***Reactive and Functional Polymers***, **114:** 127-135.
34. R. Araga, S. Soni, C. S. Sharma, (2017) Fluoride adsorption from aqueous solution using activated carbon obtained from KOH-treated jamun (*Syzygium cumini*) seed, ***Journal of Environmental Chemical Engineering***, **5:** 5608-5616.
35. A. Ramdani, S. Taleb, A. Benghalem, N. Ghaffour, (2010) Removal of excess fluoride ions from Saharan brackish water by adsorption on natural materials, ***Desalination***, **250:** 408-413.
36. P. Zhu, H. Wang, B. Sun, P. Deng, S. Hou, Y. Yu, (2009) Adsorption of fluoride from aqueous solution by magnesia-amended silicon dioxide granules, ***Journal of Chemical Technology and Biotechnology***, **84:** 1449-1455.
37. S. Lagergren, (1898) About the theory of so-called adsorption of soluble substances, ***Kungliga Svenska Vetenskapsakademiens Handlingar***, **24:** 1-39.
38. Y. S. Ho, G. McKay, (1999) Pseudo-second order model for sorption processes, ***Process Biochemistry,*** **34:** 451-465.
39. W. J. Weber, J. C. Morris, (1963) Kinetics of adsorption on carbon from solution, ***Journal of the Sanitary Engineering Divison***, **89:** 31-60.
40. P. S. Rao, Y. Vijaya, V. M. Boddu, A. Krishnaiah, (2009) Adsorptive removal of copper and nickel ions from water using chitosan coated PVC beads, ***Bioresource Technology***, **100:** 194-199.
41. I. Langmuir, (1916) The constitution and fundamental properties of solids and liquids, ***Journal of the American Chemical Society***, **38:** 2221-2295.
42. T. W. Weber, P. K. Chakravorti, (1974) Pore and solid diffusion models for fixed adsorbors, ***AIChE Journal***, **20:** 226-237.
43. Z. Zhang, Y. Tan, M. Zhong, (2011) Defluorination of wastewater by calcium chloride modified natural zeolite, ***Desalination***, **276:** 246-252.
44. S. M. Maliyekkal, A. K. Sharma, L. Philip, (2006) Manganese-oxide-coated alumina: A promising sorbent for defluoridation of water, ***Water Research***, **40:** 3497-3506.
45. A. Bansiwal, D. Thakre, N. Labhshetwar, S. Meshram, S. Rayalu, (2009) Fluoride removal using lanthanum incorporated chitosan beads, ***Colloids and Surfaces B: Biointerfaces***, **74:** 216-224.
46. A. Bansiwal, P. Pillewan, R. B. Biniwale, S. S. Rayalu, (2010) Copper oxide incorporated mesoporous alumina for defluoridation of drinking water, ***Microporous Mesoporous Materials***, **129:** 54-61.
47. S. Jagtap, K. K. N. Yenkie, N. Labhsetwar, S. Rayalu, (2011) Defluoridation of drinking water using chitosan based mesoporous alumina, ***Microporous Mesoporous Materials***, **142:** 454-463.
48. A. A. M. Daifullah, S. M. Yakout, S. A. Flreefy, (2007) Adsorption of fluoride in aqueous solutions using $KMno_4$-modified activated carbon derived from steam pyrolysis of rice straw, ***Journal of Hazardous Materials***, **147:** 633-643.
49. W. Liang, L. Zhan, L. Piao, C. Russel, (2011) Fluoride removal performance of glass derived hydroxyapatite, ***Materials Research Bulletin***, **46:** 205-209.
50. R. Yao, F. Meng, L. Zhang, D. Ma, M. Wang, (2009) Defluoridation of water using neodymium-modified chitosan, ***Journal of Hazardous Materials***, **165:** 454-460.
51. R. S. Sathish, S. Sairam, V. G. Raja, G. N. Rao, C. Janardhana, (2008) Defluoridation of water using zirconium impregnated coconut fiber carbon, ***Separation Science and Technology***, **43:** 3676-3694.
52. J. Zhang, S. Xie, Y. S. Ho, (2009) Removal of fluoride ions from aqueous solution using modified attapulgite as adsorbent, ***Journal of Hazardous Materials***, **165:** 218-222.
53. H. M. F. Freundlich, (1906) Over the Adsorption in solution, ***The Journal of Physical Chemistry***, **57:** 385-471.